Hybrid dynamic control of a sewage sludge dewatering and incineration process

Steffen Ruppert[1], Christian Stöcker[2], Markus Koitka[2], Peter Schmittel[2] and Julien Provost[1]

***Abstract*— This paper deals with the automatic setting of setpoints for physically interconnected decentralized control loops in dependence upon the overall plant operating mode, denoted as high-level control. In the last two decades, a lot of effort has been spent on the development of such control concepts which are almost exclusively based on online-optimization, like Model Predictive Control (MPC). The application of these optimization based control approaches at a real plant is cost-intensive and, therefore, economically viable for large-scale processes only. However, in the process industry there is also a need for high-level control concepts for less sophisticated processes, which are characterized by a *weak meshing* of the decentralized control loops. This paper proposes a new hybrid dynamic controller for the automatic setpoint setting for an industrial sewage sludge dewatering and incineration process and compares its behavior with an MPC in a simulation study. The investigation shows that the hybrid controller yields good results by adapting the setpoints to different plant operation modes and, moreover, even approximates the behavior of the MPC with appropriate accuracy. This example illustrates the great potential of the proposed approach for industrial applications where cost efficiency and effortless maintenance are important.**

I. Introduction

Since many years the process industry pushes further automation of the production processes with various aims, like the optimization of throughput, improvement of energy efficiency, or reduction of manual handling operations. The majority of the overall processes consists of interconnected subsystems, where the subsystems are usually controlled in a decentralized manner. Although a decentralized control structure might not be optimal from a process control perspective, it is justified by different reasons (e. g. some subsystems are units which include a controller provided by the vendor and a decentralized control reduces complexity in the engineering) and, hence, is a given for many existing plants. The consequence of this control structure is that the setpoints of the individual controllers need to be coordinated and adapted to changing plant operation modes, which is typically done by one or several human operators. This task however is rather complex, due to the physical interconnections of the subsystems and hard constraints on process and control variables. Thus, the manual specification of the setpoints for the controllers generally yields suboptimal results. Such problems have already been addressed by plant-wide controls which suggest a hierarchical control structure where production goals equal control objectives [1], [2]. Breaking down the control objectives level by level is synchronizing the plant's operation. The setpoints of the lower level are adjusted by the higher level [3]. This composition admits opportunities for optimization-based high-level controllers that automatically adjust the setpoints of the decentralized controllers to the current plant operation mode.

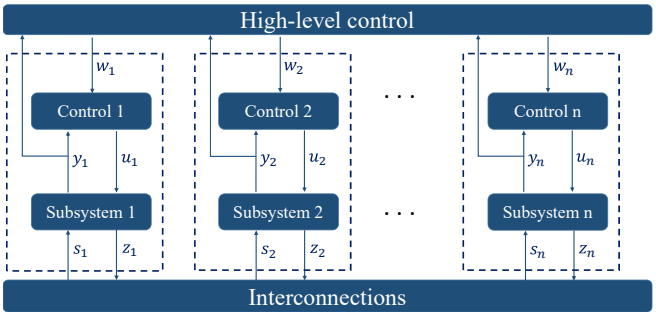

Fig. 1. High level control with decentralized controls

The aim of the high-level control can be described as an optimal control problem

$$\boldsymbol{w}(t) = \arg\min_{\boldsymbol{w}(t)} J(\boldsymbol{x}(t), \boldsymbol{w}(t)) \tag{1a}$$

$$\text{s. t.} \quad J(\boldsymbol{x}(t), \boldsymbol{w}(t)) = \int_0^{T_\mathrm{e}} h(\boldsymbol{x}(t), \boldsymbol{w}(t))\mathrm{d}t \tag{1b}$$

with the plant state $\boldsymbol{x} \in \mathcal{X} \subset \mathcal{R}^n$ and the control setpoints $\boldsymbol{w} \in \mathcal{W} \subset \mathcal{R}^m$. Well-elaborated and expedient approaches to the problem (1) are optimization based control concepts, such as MPC and Real Time Optimization (RTO), which are successfully implemented in power plant, petroleum and chemical industry [4], [5]. MPC uses a time-discrete dynamic plant model and solves the discretized version of (1) at each control interval predicting a sequence for future manipulated variables to optimize the plant behavior [6], [7]. In industrial applications, MPC is mostly based on linear dynamic models whereas RTO uses an extensive rigorous non-linear process model to optimize the behavior aiming at a steady state of the process [8]. Also, there exist effective combinations of RTO and MPC where the MPC targets are adjusted by the RTO optimizing the dynamic behavior in non-linear processes [9]. Another interesting highly sophisticating approach is the explicit MPC where the optimization problem is solved offline in a multiparametrical manner for given operating conditions in order to simplify the online control operations and to shorten response times [10].

In practical applications, however, the implementation of the described control concepts has some disadvantages: it

[1]Steffen Ruppert and Julien Provost are with the Technical University of Munich, Garching, Germany provost@ses.mw.tum.de

[2]Christian Stöcker, Markus Koitka and Peter Schmittel are with BASF SE, Ludwigshafen, Germany christian.stoecker@basf.com

entails high costs for investment, is not implemented directly in the distribution control systems, has to be reconfigurated with plant changes, and requires special knowledge of control engineers in engineering and maintenance. For these reasons, MPC might not be an economic solution for a class of systems which are *weakly meshed* (as defined in Sec. II).

Notwithstanding that optimization based controls are unsuitable for particular practical high-level control problems, the process industry has a demand for tailored solutions in these cases. This paper points out to the need in process industry for alternative high-level control approaches to MPC and, by this, pursues three aims:

- It specifies the class of control problems of the form (1), where the use of optimization based control is typically uneconomical.
- It presents a benchmark problem (control of the dewatering and incineration of sewage sludge at a waste water treatment plant), proposes a hybrid dynamical high-level controller, and contrasts this concept with an MPC in simulations.
- It derives from the comparison of the two approaches interesting and important research questions concerning the development of novel high-level control approaches besides optimization based controls.

Thus, the aim of this paper is to proof a satisfying approximation of these advanced control concepts by hybrid dynamic controls which are more economic and undemanding to implement.

The remainder of this paper is organized as follows: in section II, the control problem is generally described and concretized. The benchmark problem of the sewage sludge dewatering and incineration is introduced in Sec. III, before two approaches to high-level control - MPC and a hybrid dynamical controller - are proposed in Sec. IV, which are then compared and analyzed by simulations in Sec. IV. The paper closes with interesting questions and observations that are derived from the results of the simulations and which motivate further research.

II. Problem statement

As previously explained, this paper deals with the high-level control of interconnected systems with decentralized controllers, which are characterized as *weakly meshed*. This problem statement is substantiated in this section, starting with the definition of *weakly meshed* systems.

Consider a process consisting of N physically interconnected subsystems, where each subsystem is controlled in a decentralized manner by a separate controller. The behavior of the controlled subsystem Σ_i is described by

$$\Sigma_i : \begin{cases} \dot{\boldsymbol{x}}_i(t) = \boldsymbol{f}_i(\boldsymbol{x}_i(t), s_i(t), \boldsymbol{d}_i(t), \boldsymbol{w}_i(t)), \\ \boldsymbol{x}_i(0) = \boldsymbol{x}_{i,0}, \\ \boldsymbol{y}_i(t) = \boldsymbol{g}_{\mathrm{y},i}(\boldsymbol{x}_i(t), s_i(t), \boldsymbol{d}_i(t)), \\ z_i(t) = \boldsymbol{g}_{\mathrm{z},i}(\boldsymbol{x}_i(t), s_i(t), \boldsymbol{d}_i(t)) \end{cases} \tag{2}$$

where $\boldsymbol{x}_i \in \mathcal{X}_i \subset \mathbb{R}^{n_i}$ denotes the state, $\boldsymbol{y}_i \in \mathcal{Y}_i \subset \mathbb{R}^{m_i}$ the output, $\boldsymbol{d}_i \in \mathcal{D}_i \subset \mathbb{R}^{r_i}$ the unknown but bounded disturbance, $\boldsymbol{w}_i \in \mathcal{W}_i \subset \mathbb{R}^{m_i}$ the setpoint reference, $s_i \in \mathcal{S}_i \subset \mathbb{R}$ the coupling input, and $z_i \in \mathcal{Z}_i \subset \mathbb{R}$ the coupling output. The coupling input $s_i(t)$ is determined according to the equation

$$s_i(t) = \boldsymbol{\phi}_i(z_1(t), \cdots, z_N(t)) \tag{3}$$

with the coupling relation $\phi_i : \mathcal{Z}_1 \times \cdots \times \mathcal{Z}_N \to \mathcal{S}_i$.

Now regard the decentrally controlled subsystems (2) together with the interconnections (3) as a network, that is described as a graph $G = (V, E)$ where subsystem Σ_i is represented by the vertice $v_i \in V, (i \in \{1, \cdots, N\})$ and the direct influence of subsystem Σ_j on Σ_i by the unweighted, but directed edge (v_j, v_i). v_i is called the head and v_j is called the tail of the edge (v_j, v_i). Note that for a graph G, $d_G^-(v_i)$ and $d_G^+(v_i)$ denote the indegree (number of head ends adjacent to v_i) or the outdegree (number of tail ends adjacent to v_i) of v_i, respectively.

With this notion, the term of *weakly meshed* systems, as investigated in this paper, can be defined.

Definition 2.1: Consider the graph G that is derived from the structure of the decentrally controlled subsystems (2) with the interconnections (3) for all $i = 1, \cdots, N$. The overall system is called *weakly meshed* if G satisfies the conditions

$$\max(d_G^-(v_i)) \leq 2, \tag{4a}$$

$$\max(d_G^+(v_i)) \leq 2 \tag{4b}$$

for all $i = 1, \cdots, N$.

These two conditions in the definition of *weakly meshed* systems can be interpreted as follows: No subsystem is directly influenced by more than two other subsystems and each subsystem has a direct impact on not more than two other subsystems which together is a restriction on the meshing of the network.

With this definition, the problem statement can now be made concrete.

Problem 2.1: Consider a network of N physically interconnected and decentrally controlled subsystems (2) together with the interconnections (3). The graph, derived from this system, satisfies the conditions (4a), (4b). Find a high-level controller $\mathcal{C}$ that specifies the reference value $\boldsymbol{w}_i$ for all decentralized controllers $(i = 1, \cdots, N)$ in accordance with (1) and does not use online-optimization based methods.

III. Benchmark problem

The proposed benchmark problem is the process of the dewatering and incineration of sewage sludge at a real large-scale industrial waste water treatment plant (WWTP), which fulfills the conditions of the Problem 2.1. The sewage sludge is a byproduct of the sewage treatment process, which is not considered in this benchmark problem. For detailed information on the sewage treatment process, the reader is referred to [11]. Subsequently, the dewatering and incineration process (DIP) is described.

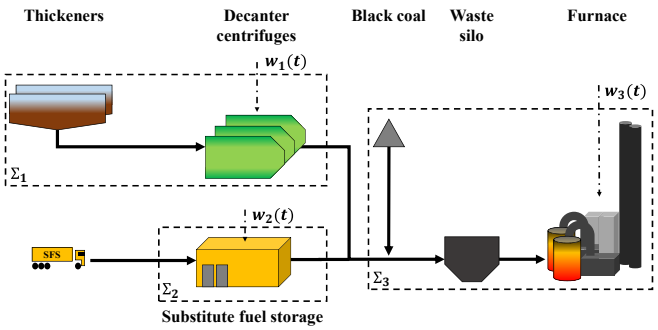

Fig. 2. Sewage sludge dewatering and incineration processes

A. Technical description of the DIP

The DIP, illustrated in Fig. 2, is divided into the three subsystems which are explained in the following.

Dewatering system. Sewage sludge consists of two components, surplus sludge (SS) and primary sludge (PS). The total sludge is directed into six thickeners for dewatering. Therefrom it is conducted into decanter centrifuges which separate the solid material from the liquids. The liquid is recycled into the sewage treatment process while the solid (denoted as decanter output) is discharged on a trough chain conveyor. The mass flow of the decanter output is controlled by a subordinate decanter control that takes a setpoint reference $w_1(t)$.

Substitute fuel storage. Since the burning capacity of the furnace exceeds the mass produced in the sewage treatment process, additional material (denoted as substitute fuel) is incinerated in the system as well. The substitute fuel is delivered into the substitute fuel storage (SFS) and from there transported via a discharge screw on the through chain conveyor where it is merged with the decanter output. The mass flow of the substitute fuel on the conveyor is controlled by the rotation speed of the discharge screw that can be specified by the setpoint $w_2(t)$.

Incineration. The decanter output together with the substitute fuel is mixed with black coal on the trough chain conveyor in order to increase the overall heating value. This mixture (denoted as waste) is directed into a waste silo. From here the waste is conveyed into the furnace. The incineration process is controlled by a subordinate controller and is mainly influenced by the mass flow into the furnace that can be specified by the setpoint $w_3(t)$.

B. Mathematical model of the DIP

The dewatering system Σ_1, i. e. the thickeners together with the controlled decanter centrifuges, is described by the state-space model

$$\dot{x}_1(t) = -w_1(t) + \begin{pmatrix}\gamma_{11}(t) & \gamma_{12}(t)\end{pmatrix}\begin{pmatrix}d_{11}(t)\\ d_{12}(t)\end{pmatrix} \tag{5a}$$

$$y_1(t) = \big(\gamma_{13}(t)C_1\big)^{-1}x_1(t) \tag{5b}$$

$$z_1(t) = \big(\gamma_{14}(t)\big)^{-1}w_1(t) \tag{5c}$$

where $x_1(t)$ is the total mass of sewage sludge in the thickeners, $w_1(t)$ is the mass discharged by the decanter centrifuges, and $d_{11}(t)$ and $d_{12}(t)$ denote the feed into the thickeners of SS or PS, respectively. Both inflows are unknown and, thus, modeled as disturbances. Note that the solid contents $\gamma_{11}(t)$ and $\gamma_{12}(t)$ of the flows $d_{11}(t)$ and $d_{12}(t)$, respectively, are time-varying due to changing compositions of the waste water. Accordingly the solid content of the sludge in the thickener $\gamma_{13}(t)$ is a time-varying disturbance. C_1 denotes the volume capacity of the thickeners. $\gamma_{14}(t)$ is the solid content of the decanter output and is defined by the function

$$\gamma_{14}(t) = -24w_1(t) - 0.2\gamma_{15}(t) + 40 \tag{6}$$

that covers unmodeled effects in the solid-liquid separation which have an impact on the decanter output quality. In (6), $\gamma_{15}(t)$ is the varying percentage of total organic solids which can be regarded as a disturbance on the sludge quality.

The SFS Σ_2 is represented by the state-space model

$$\dot{x}_2(t) = -w_2(t) + d_2(t) \tag{7a}$$

$$y_2(t) = x_2(t) \tag{7b}$$

$$z_2(t) = w_2(t) \tag{7c}$$

where $x_2(t)$ is the total mass of substitute fuel, $w_2(t)$ is the substitute fuel flow out of the storage, and $d_2(t)$ is the supplied substitute fuel.

The incineration Σ_3 is described by

$$\dot{x}_3(t) = -k_c w_3(t) + \xi_3 s_3(t - \mathrm{T}_3) \tag{8a}$$

$$y_3(t) = x_3(t) \tag{8b}$$

where $x_3(t)$ denotes the mass in the waste silo, the air flow setpoint of the furnace $w_3(t)$ multiplied by k_c, which is defined as $6.5 \cdot 10^{-4}$, equals the waste mass flow into the furnace, and $s_3(t)$ represents the feed into the waste silo. The amount of black coal added to the waste corresponds to 10% of the waste mass which is covered by $\xi_3 = 1.1$. T_3 conforms to the transport delay of the feed due to the layout of the subsystems.

Finally, the coupling matrix which describes the interconnection of the subsystems is given by

$$\begin{pmatrix}s_1(t)\\ s_2(t)\\ s_3(t)\end{pmatrix} = \begin{pmatrix}0 & 0 & 0\\ 0 & 0 & 0\\ 1 & 1 & 0\end{pmatrix}\begin{pmatrix}z_1(t)\\ z_2(t)\\ z_3(t)\end{pmatrix} \tag{9}$$

Note that the DIP is *weakly meshed* in the sense of Def. 2.1, since Σ_3 is only influenced by subsystems Σ_1 and Σ_2, which yields $d_G^+(v_3) = 2$, and Σ_1 and Σ_2 have no interconnection such that $d_G^-(v_1) = d_G^-(v_2) = 1$ holds. All other indegrees and outdegrees are vanishing.

C. Benchmark control problem

The aim of the high-level controller for the DIP is to balance and orchestrate the mass flows from the dewatering system and the substitute fuel storage as well as the throughput of waste into the incineration such that the subsystems' process variables remain in a bounded surrounding of a predefined reference value under all operating conditions,

considering the constraints on process and control variables. Referring to Eq. (1), this objective can be formally described by an optimal control problem with an appropriately defined cost function

$$J = \sum_{j=1}^{\mathrm{t}_p} \big\{ \eta_1 (\hat{w}_1 - y_1[k+j])^2 + \eta_2 (\hat{w}_2 - y_2[k+j])^2 + \eta_3 (\hat{w}_3 - y_3[k+j])^2 \big\} \tag{10}$$

where the squared control deviation $(\hat{w}_i - y_i[k+j])^2$ is weighted by the respective parameter η_i for $i \in \{1,2,3\}$ and the prediction horizon is represented by t_p.
However, according to the requirements in the problem statement 2.1 this contribution strives for a non-online optimization based solution for the high-level control. To this end, the control aim is reformulated using the notion of practical stability [12]:

Problem statement for the high-level control of the DIP: Determine the setpoint reference $w_i(t) \in \mathcal{W}_i$ for all $i \in \{1,2,3\}$ such that the system (5)–(9) is practically stable:

$$y_i(t) \in \Omega_i := \big\{ y_i \in \mathbb{R}^{m_i} \big| y_{\min i} \le y_i \le y_{\max i} \big\}, \quad \forall t \ge 0, i \in \{1,2,3\}. \tag{11}$$

The lower limit $y_{\min i}$ and the upper limit $y_{\max i}$ span the allowed range for each $y_i(t)$. The constraints for the feasible setpoints are defined accordingly:

$$\mathcal{W}_i := \big\{ w_i \in \mathbb{R}^{m_i} \big| w_{\min i} \le w_i \le w_{i\max i} \big\}, \quad \forall t \ge 0, i \in \{1,2,3\}. \tag{12}$$

The values for the upper and lower limits of the process and control variables are summarized in Table I.

Subsystem	$y_{\min i}$	$y_{\max i}$	$w_{\min i}$	$w_{\max i}$
Σ_1	20%	70%	0 t/min	0.208 t/min
Σ_2	200 t	2500 t	0 t/min	1.3 t/min
Σ_3	80 t	480 t	37 kN m^3/h	51 kN m^3/h

TABLE I
LIMITS OF THE PROCESS AND CONTROL VARIABLES

IV. HIGH-LEVEL CONTROL DESIGN

In this section a solution to the problem of a high-level controller for the DIP is proposed, based upon an approach to hybrid dynamic control. The underlying design idea for this high-level controller $\mathcal{C}$ is that:

- in the nominal operating mode, the setpoint for each subsystem Σ_i is determined locally, i. e. by means of decentralized decision units $\mathcal{C}_i$ (for $i \in \{1,2,3\}$), and
- whenever the system tends towards an abnormal state, information links between the decision units are closed and the setpoints for all subsystems are generated in a cooperative manner.

This control strategy is inspired by a work on control over wireless networks [13], where the situation-dependent coupling between the controllers is motivated by restrictions on power consumption for information transmissions. However, its adaption to the setpoint setting for interconnected decentralized control loops to adjust the controller behavior to the operating mode is new. The design of the hybrid dynamic controller (HDC) is presented in the following paragraph.

Consider that the control aim, specified in paragraph III-C, is assumed to be best accomplished by an MPC which will be used in Sec. V as a benchmark for the HDC. The design parameters of the MPC are given in paragraph IV-B.

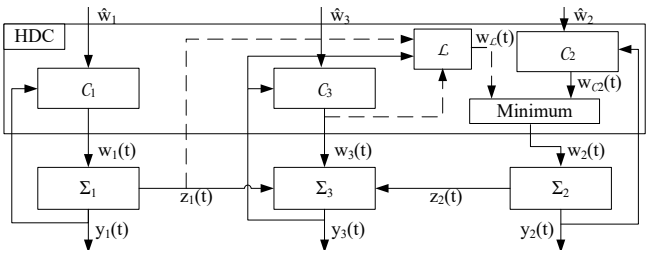

Fig. 3. Hybrid dynamic control composition

A. Hybrid dynamic control

The proposed approach to the high-level control of the DIP is a HDC, illustrated in Fig. 3, which consists of a decision unit $\mathcal{C}_i$ for each subsystem Σ_i and a switching logic $\mathcal{L}$ that generates the signal $\zeta \in \{0,1\}$, indicating the operating mode of the controller. In dependence upon the operation mode, the setpoint $w_2(t)$ is either determined in a decentralized manner (if $\zeta = 0$) or cooperatively (if $\zeta = 1$). The latter case is realized by a situation-dependent information coupling between the decision units $\mathcal{C}_i$, which is explained in more detail hereafter.
Let $e_i(t) = \hat{w}_i - y_i(t)$ denotes the deviation of the output $y_i(t)$ from a predefined reference value $\hat{w}_i$ for subsystem Σ_i. Then, the HDC is described by

$$\frac{\mathrm{d}}{\mathrm{d}t} \begin{pmatrix} x_{\mathrm{s}1}(t) \\ x_{\mathrm{s}2}(t) \\ x_{\mathrm{s}3}(t) \end{pmatrix} = \begin{pmatrix} k_{\mathrm{I}1} & 0 & 0 \\ 0 & k_{\mathrm{I}2} & 0 \\ 0 & 0 & k_{\mathrm{I}3} \end{pmatrix} \begin{pmatrix} e_1(t) \\ e_2(t) \\ e_3(t) \end{pmatrix} \tag{13a}$$

$$\begin{pmatrix} w_1(t) \\ w_{\mathcal{C}2}(t) \\ w_3(t) \\ w_{\mathcal{L}}(t) \end{pmatrix} = \begin{pmatrix} 1 & 0 & 0 \\ 0 & 1 & 0 \\ 0 & 0 & 1 \\ 0 & 0 & k_{\mathrm{c}}\zeta \end{pmatrix} \begin{pmatrix} x_{\mathrm{s}1}(t) \\ x_{\mathrm{s}2}(t) \\ x_{\mathrm{s}3}(t) \end{pmatrix} + \begin{pmatrix} k_{\mathrm{P}1} & 0 & 0 \\ 0 & k_{\mathrm{P}2} & 0 \\ 0 & 0 & k_{\mathrm{P}3} \\ 0 & 0 & k_{\mathrm{c}}k_{\mathrm{P}3}\zeta \end{pmatrix} \begin{pmatrix} e_1(t) \\ e_2(t) \\ e_3(t) \end{pmatrix} - \begin{pmatrix} 0 \\ 0 \\ 0 \\ \zeta \end{pmatrix} z_1(t) \tag{13b}$$

$$w_2(t) = \begin{cases} w_{\mathcal{C}2}(t) & \text{for } \zeta = 0 \\ \min\big(w_{\mathcal{C}2}(t); w_{\mathcal{L}}(t)\big) & \text{for } \zeta = 1 \end{cases} \tag{13c}$$

with initial controller state $x_{si}(0) = 0$ for all $i \in \{1, 2, 3\}$, together with the switching logic

$$\mathcal{L}: \quad \zeta = \begin{cases} 1 & \text{if } y_3 \geq 336 \text{ t} \\ 0 & \text{if } y_3 \leq 288 \text{ t}. \end{cases} \tag{13d}$$

The switching logic behaves like a bang-bang controller that switches on if the mass $y_3(t)$ in the waste silo exceeds 336 t and switches off if $y_3(t)$ falls below 228 t. The chosen hysteresis gap ensures that a Zeno behavior, i. e. an infinite switching of the modes in finite time, is excluded.

Note that the decision units $\mathcal{C}_1$, $\mathcal{C}_2$ and $\mathcal{C}_3$, which generate the signals $w_1(t)$, $w_{\mathcal{C}2}(t)$ $w_3(t)$, respectively, are designed as PI-controllers with appropriately chosen proportional gains $k_{\mathrm{P}i}$ and integral gains $k_{\mathrm{I}i}$ (Table II). For $\zeta = 0$, $w_2(t)$ is built by the PI-controller $\mathcal{C}_2$ with the respective gains, while for $\zeta = 1$ $w_2(t)$ reduces to the minimum of the PI-controller generated $w_{\mathcal{C}2}(t)$ and the switching logic $\mathcal{L}$ built

$$w_{\mathcal{L}}(t) = k_{\mathrm{c}}\big(x_{\mathrm{s}3}(t) + k_{\mathrm{P}3}e_3(t)\big) - z_1(t) \tag{14}$$
$$= k_{\mathrm{c}}w_3(t) - z_1(t) \tag{15}$$

with the coefficient k_{c}, describing the relation between the setpoint $w_3(t)$ for the furnace air flow and the burned mass of waste. More precisely, the reference $w_{\mathcal{L}}(t)$ is adapted to the decanter output $z_1(t)$ such that the total conveyed waste is limited to the reference $k_{\mathrm{c}}w_3(t)$ of the mass to be incinerated. According to this control law, the decision unit $\mathcal{C}_2$ together with the switching logic $\mathcal{L}$ ensure that, in case the mass $y_3(t)$ in the waste silo exceeds a certain level, the setpoint $w_2(t)$ for the feed of substitute fuel is reduced and guarantees that in mode $\zeta = 1$ the mass $y_3(t)$ cannot increase. A decrease of the mass $y_3(t)$ in the waste silo requires either a lower decanter output $z_1(t)$ or a substitute fuel discharge setpoint $w_{\mathcal{C}2}(t)$ lower than $w_{\mathcal{L}}(t)$. Accordingly the waste mass falls below 228 t and switching logic $\mathcal{L}$ changes into mode $\zeta = 0$.

Parameters	$\mathcal{C}_1$	$\mathcal{C}_2$	$\mathcal{C}_3$
k_P	$-1.2 \cdot 10^{-3}$	$-3.5 \cdot 10^{-3}$	$-30 \cdot 10^{-3}$
k_I	$-5 \cdot 10^{-7}$	-10^{-6}	$-2 \cdot 10^{-6}$

TABLE II
HDC SETTING

B. Model predictive control

An MPC is assumed to yield optimal results on the setpoint setting for the DIP, but its implementation at the real plant is unfavorable due to high costs for engineering and maintenance. However, for the purpose of evaluating the functionality of the proposed HDC, a linear MPC is used as benchmark. The applied MPC includes a linearized model of the DIP which is obtained by replacing the time-varying disturbances by respective constant values shown in Table III. The chosen objective function is of the form (10) with weights $\eta_1 = 100$, $\eta_2 = 0.02$ and $\eta_3 = 15$ what underlines the importance of subsystem Σ_1 and leaves the MPC enough leeway regarding subsystem Σ_2. The prediction horizon t_p is set to 350 time steps which follows the design suggestion of [7] and the control horizon, i. e. the update rate of the output of the MPC, is chosen to be 20 minutes with respect to the time constants of the process.

d_{11}	γ_{11}	d_{12}	γ_{12}	γ_{13}	γ_{15}	d_2
16.7	$4.8 \cdot 10^{-3}$	6.8	$8.5 \cdot 10^{-3}$	3	50	0.42

TABLE III
MPC SETTING

V. Simulative comparison and evaluation of the control concepts

This section focuses on the comparison of the HDC to the MPC on their behavior in specific test cases. Every test case is described as simulation scenario lasting 30 days. Due to the defined optimal behavior of the MPC the deviating behavior of the HDC is analyzed.

A. Performance indicator

For evaluating the HDC behavior to the MPC, the performance indicator δ is defined which describes the deviating behavior of the HDC to the MPC in relation to the overall MPC behavior:

$$\delta = \frac{\int_0^t \|\bar{\lambda}_{\mathrm{i}}(t) - \lambda_{\mathrm{i}}(t)\| \,\mathrm{d}t}{\int_0^t \lambda_{\mathrm{i}}(t) \,\mathrm{d}t} \qquad t \in [0, 42300] \tag{16}$$

For the HDC the variable $\bar{\lambda}_{\mathrm{i}}(t)$ and for the MPC the variable $\lambda_{\mathrm{i}}(t)$ represent the respective setpoint $w_i(t)$ or control variable $y_i(t)$ of the subsystem Σ_i with $i \in \{1, 2, 3\}$. The time interval $t \in [0, 42300]$ conforms to 30 days in minutes.

B. Test cases

The following five test cases were developed and analyzed:

1) Standard operating conditions (SOC): The standard operating conditions are described by the SS inflow $d_{11}(t)$ and the PS inflow $d_{12}(t)$ and their respective total solids contents $\gamma_{11}(t)$ and $\gamma_{12}(t)$ which are derived by historical data of the industrial WWTP. The solid content of the thickener sludge $\gamma_{13}(t)$ and the organic total solids $\gamma_{15}(t)$ are presented as disturbances as well as the substitute fuel inflow $d_2(t)$:

$$d_{11}(t) = 16.7 + 1.5 \ \sin(6 \cdot 10^{-4}t) \tag{17}$$
$$\gamma_{11}(t) = 4.8 \cdot 10^{-3} \tag{18}$$
$$d_{12}(t) = 6.8 \tag{19}$$
$$\gamma_{12}(t) = 8.5 \cdot 10^{-3} + 5.5 \cdot 10^{-3} \ \sin(14.5 \cdot 10^{-4}t + \frac{\pi}{2}) \tag{20}$$
$$\gamma_{13}(t) = 3 + 0.2 \ \sin(5 \cdot 10^{-4}t) \tag{21}$$
$$\gamma_{15}(t) = 50 + 10 \ \sin(5 \cdot 10^{-4}t + \frac{\pi}{2}) \tag{22}$$
$$d_2(t) = 0.42 \tag{23}$$

2) Heavy rain (HR): This test case describes a heavy rain event which results in an increased PS inflow $d_{12}(t)$ lasting for one day. Apart from these changes standard operating conditions prevail.

$$d_{12}(t) = 26.1 \tag{24}$$

3) Reduction of surplus sludge(RSS): In specific circumstances SS is bisected for process reasons. The reduction of SS $d_{11}(t)$ lasts for 7 days. Apart from these changes standard operating conditions prevail.

$$d_{11}(t) = 8.75 + 1.5 \quad \sin(6 \cdot 10^{-4} t) \tag{25}$$

4) Incinerator shutdown preparation(ISD): For maintenance or asset improvements the incineration is shut down. Preparing this, high safety capacities in the sewage treatment processes are provided what results in an increased inflow of SS $d_{11}(t)$ for 7 days. Apart from these changes standard operating conditions prevail.

$$d_{11}(t) = 26.7 + 1.5 \quad \sin(6 \cdot 10^{-4} t) \tag{26}$$

5) Decreased heating value(DHV): This case covers a heating value decrease of the waste burned what leads to a lower furnace burning capacity for 7 days. Apart from these changes standard operating conditions prevail.

C. Evaluation of the simulation results

In the following, the results of test cases *SOC* and *HR* (see Fig. 4) are presented in detail. For room reasons, the results of the other test cases are summarized in the Table IV.

System variables	SOC	HR	RSS	ISD	DHV
y_1	7.8	8.9	8.1	8.2	7.6
w_1	13	14.1	13	10	10.6
y_2	2.9	5.5	3.5	4	8.4
w_2	6.4	10	4.3	8.3	10.4
y_3	28.2	30.8	33.3	29.8	27
w_3	8.1	7	5.2	5.9	8

TABLE IV

PERFORMANCE INDICATOR δ IN %

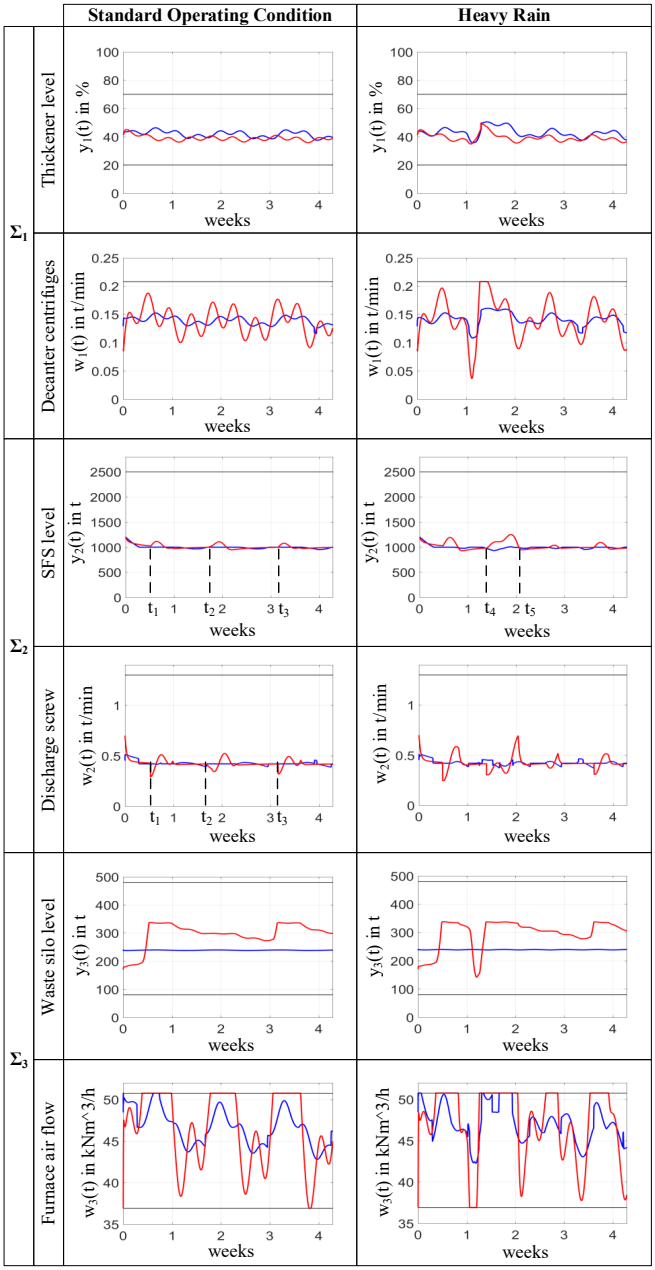

Fig. 4. Standard Operating Condition (left column) and Heavy Rain (right column): MPC (blue) and HDC (red)

1) Discussion of SOC: In the left box, the dewatering system's behavior is demonstrated where the thickener behavior in the upper graph shows a satisfying approach of the setpoint $\hat{w}_1$ for both control concepts. In the lower graph, the adjustment of the decanter centrifuges is represented where the MPC features a smoother operation. The highest deviation between the control concepts' behaviors is 0.057t/min what equals 27.7% of the setpoint range. The central box represents the SFS level in the upper graph where the setpoint $\hat{w}_2$ is well hold, however three peaks are noticed in the HDC behavior at times t_1, t_2 and t_3. This is resulting in a switch of the switching logic $\mathcal{L}$ decreasing the setpoint $w_2(t)$ monitored in the lower graph. In the upper graph of the right box, greater deviations in the silo mass $y_3(t)$ are observed which result in a change of dimensional scaling from thousands(Σ_1, Σ_2) to hundreds (Σ_3). However, the HDC never exceeds the provided system limits. The furnace air flow $w_3(t)$ shows heavier oscillations with the HDC operation. In times where $\zeta = 1$, the furnace air flow takes high values to burn the incoming waste and to reset the silo. In general, a satisfying approximation of the MPC behavior by the HDC is monitored where the control aim (11) is achieved by both control concepts, neither exceeding nor underrunning the respective limits. The performance indicators δ shown in Table IV underline this approximation of the MPC behavior by the HDC. All performance indicators δ lie

within an acceptable two-digit percent range what concludes to a proper adaption of the MPC behavior by the HDC.

2) Discussion of HR: The dewatering system Σ_1 displayed in the left box represents a strong increase of the thickener level which is the result of the almost quadrupled inflow $d_{12}(t)$. Both concepts respond to the disturbance by accelerating the decanter centrifuges shown by the rapid increase of the setpoint $w_1(t)$. Again, larger amplitudes are monitored with the HDC behavior pushing the decanter centrifuges to their limit. Note that the MPC features smoother curves in the thickener level $y_1(t)$ and the decanter centrifuges setpoint $w_1(t)$. For the HDC, the increased solid flow induces a switch in the switching logic $\mathcal{L}$ and subsequently a level increase in Σ_2 over the time interval $[\mathrm{t}_4, \mathrm{t}_5]$. The restriction of the discharge screw setpoint $w_2(t)$ is observed in the lower graph. However, the MPC manages to hold the setpoint $\hat{w}_2$ in subsystem Σ_2 almost constantly what is traced back to its prediction characteristic. Again, the waste mass in the silo $y_3(t)$ demonstrates a higher deviation between the MPC and the HDC behavior due to changing dimensional scaling, a larger incoming waste mass and an intensified oscillation of the furnace air flow $w_3(t)$. However no limit exceedings occur in both control concepts what achieves the control aim of Eq.(11). The performance indicators δ in Table IV approve a satisfying approximation of the MPC behavior by the HDC.

In summary, both control concepts maintain the given limits over all test cases. The performance indicators δ of the variables differ less over the test cases, what emphasizes that the HDC approximates the MPC behavior satisfying independently to operating conditions. These results verify the fulfillment of the control aim Eq.(11) and both control concepts are approved as *practically stable*. The obtained results confirm an adequate mimicry to MPC by hybrid dynamic controllers for *weakly meshed* systems such as the DIP. Concluding, this demonstration supports the application of hybrid dynamic controllers which are more economic in terms of implementation and maintenance costs at an acceptable loss of control performance.

VI. Conclusion and further research

This paper has investigated the setpoint setting by a high level controller for processes that consist of physically interconnected decentralized control loops, as they frequently appear in process industry. It has shown that control problems of the form (1), that foremost call for online optimization-based applications, can be solved by a hybrid dynamic control approach, i. e. the combination of classical controllers and a switching logic that determines the controller operation mode. Moreover, a comparison of both approaches by simulation has demonstrated that the hybrid dynamic controller can even approximate the behavior of the MPC. This is a very interesting result, particularly from the viewpoint of the process industry, where there is a need for such solutions for a special class of control problems that is mainly characterized by the *weak meshing* of the interconnected systems.

Hence this approach is no generic design method and the development of a methodical controller synthesis requires further research motivated by the following concluding questions:

- Can a control design method be found that derives a hybrid dynamic controller for high-level control problems in *weakly meshed* systems?
- How is the complexity of the controller linked to the meshing of the network?
- Can the restriction on the meshing as in Def. 2.1 be relaxed?

References

[1] M. Morari and G. Stephanopoulos, "Studies in the synthesis of control structures for chemical processes: Part ii: Structural aspects and the synthesis of alternative feasible control schemes," *AIChE Journal*, vol. 26, no. 2, pp. 232–246, 1980.

[2] C. S. Ng and G. Stephanopoulos, "Synthesis of control systems for chemical plants," *Computers & Chemical Engineering*, vol. 20, Supplement 2, pp. S999–S1004, 1996.

[3] T. Larsson and S. Skogestad, "Plantwide control-a review and a new design procedure," *Modeling, Identification and control*, vol. 21, no. 4, p. 209, 2000.

[4] M. Diehl, I. Uslu, R. Findeisen, S. Schwarzkopf, F. Allgöwer, H. G. Bock, T. Bürner, E. D. Gilles, A. Kienle, and J. P. Schlöder, *Real-time optimization for large scale processes: Nonlinear model predictive control of a high purity distillation column*. Springer, 2001, pp. 363–383.

[5] S. J. Qin and T. A. Badgwell, *An overview of nonlinear model predictive control applications*. Springer, 2000, pp. 369–392.

[6] J. B. Rawlings and D. Q. Mayne, *Model predictive control : theory and design*. Madison, Wis.: Nob Hill Pub., 2009.

[7] L. T. Biegler, *Nonlinear programming: concepts, algorithms, and applications to chemical processes*. SIAM, 2010.

[8] ——, "Efficient nonlinear programming algorithms for chemical process control and operations," in *IFIP Conference on System Modeling and Optimization*. Springer, Conference Proceedings, pp. 21–35.

[9] M. L. Darby, M. Nikolaou, J. Jones, and D. Nicholson, "Rto: An overview and assessment of current practice," *Journal of Process Control*, vol. 21, no. 6, pp. 874–884, 2011.

[10] A. Bemporad, F. Borrelli, and M. Morari, "Model predictive control based on linear programming the explicit solution," *IEEE Transactions on Automatic Control*, vol. 47, no. 12, pp. 1974–1985, 2002.

[11] G. Olsson and B. Newell, *Wastewater treatment systems*. IWA publishing, 1999.

[12] H. K. Khalil, *Noninear Systems*. Prentice-Hall, New Jersey, 1996.

[13] R. Schuh and J. Lunze, "Design of the communication structure of a self-organizing networked controller for heterogeneous agents," in *Control Conference (ECC), 2015 European*. IEEE, Conference Proceedings, pp. 2194–2201.